Baryogenesis from transitional *CP* violation in the early Universe

S. J. Huber,[1,*] K. Mimasu,[2,†] and J. M. No[3,4,‡]

[1]*Department of Physics and Astronomy, University of Sussex, Brighton, BN1 9QH, United Kingdom*
[2]*Department of Physics, King's College London, Strand, WC2R 2LS London, United Kingdom*
[3]*Instituto de Fisica Teorica, IFT-UAM/CSIC, Cantoblanco, 28049, Madrid, Spain*
[4]*Departamento de Fisica Teorica, Universidad Autonoma de Madrid, Cantoblanco, 28049, Madrid, Spain*

(Received 4 November 2022; accepted 29 March 2023; published 28 April 2023)

We propose a variant of electroweak-scale baryogenesis characterized by the spontaneous breaking of the charge-parity (*CP*) symmetry in the early Universe driven by the vacuum expectation value of a *CP*-odd scalar. This *CP* breaking period in the early Universe would be ended by the electroweak phase transition, with *CP* being (approximately) conserved at present, thus avoiding the stringent electric dipole moment experimental constraints on beyond-the-Standard-Model sources of *CP* violation. We study an explicit realization via a nonminimal Higgs sector consisting of two Higgs doublets and a singlet pseudoscalar (2HDM + a). We analyze the region of the 2HDM + a parameter space where such an early Universe period of *CP* violation occurs, and show that the required thermal history and successful baryogenesis lead to a predictive scenario, testable by a combination of LHC searches and low-energy flavor measurements.

DOI: 10.1103/PhysRevD.107.075042

I. INTRODUCTION

Charge-parity (*CP*) is an approximate symmetry of Nature, only broken in the Standard Model (SM) by mixing in the fermion sector and the presence of three families of quarks and/or leptons [1,2]. The presence of *CP* violation in the early Universe, together with baryon number violation (which occurs at high temperature in the SM [3] via sphaleron processes) and a departure from thermal equilibrium, is required to generate the observed baryon asymmetry of the Universe (BAU) [4–8]. Although the amount of *CP* violation present in the SM is well known to be insufficient for the generation of the BAU (baryogenesis) at the electroweak (EW) scale [9–11], new sources of *CP* violation beyond the SM are tightly constrained by experimental searches of electric dipole moments (EDM) of the electron [12], neutron [13] and atomic elements like mercury [14]. This constitutes a severe problem for the feasibility of scenarios for EW baryogenesis.

However, such tension between successful EW baryogenesis and current experimental EDM constraints could be circumvented by a period of spontaneous *CP* breaking in the early Universe, which would act as a catalyzer for baryogenesis. Then, the absence of new sources of *CP* violation beyond the SM at present times would naturally avoid the EDM limits.[1] We show in this paper that this setup can be easily accommodated by a suitable extension of the SM Higgs sector (see also [21,22] for related scenarios). Furthermore, such a nonminimal Higgs sector can, at the same time, yield a strongly first-order EW phase transition (see e.g. [23–28]), providing the departure from thermal equilibrium needed for baryogenesis.

Specifically, we consider a two-Higgs-doublet model (2HDM) with an additional $SU(2)_L$-singlet pseudoscalar a (2HDM + a). This model has been considered recently as a well-motivated portal to dark matter (DM) [29–34], and we will discuss the resulting interplay between baryogenesis and DM in an upcoming work [35], focusing here purely on achieving baryogenesis. In our setup, a vacuum expectation value (vev) of the pseudoscalar a in the early Universe triggers the spontaneous breaking of *CP*. *CP* is then restored after the EW phase transition, which is first-order from the existence of a potential barrier between the *CP* violating (CPV) and EW minima. We refer to this setup as *transitional CP* violation. The region of parameter space that accommodates this thermal history of the Universe and

*S.Huber@sussex.ac.uk
†ken.mimasu@kcl.ac.uk
‡josemiguel.no@uam.es

[1]See [15–20] for other weak-scale baryogenesis setups which avoid current EDM experimental constraints via suppressed beyond the SM contributions to EDMs.

leads to successful baryogenesis leaves no trace in current EDM experiments, but can be probed via current/future LHC searches and (possibly) via low-energy flavor experiments (rare B-meson decays).

II. 2HDM + a

Let us begin with the scalar potential for the model, $V = V_{\rm 2HDM} + V_a$. $V_{\rm 2HDM}$ is the 2HDM scalar potential for the two Higgs doublets $H_{1,2}$ with a softly broken $\mathbb{Z}_2$ symmetry:

$$\begin{aligned} V_{\rm 2HDM} = {} & \mu_1^2|H_1|^2 + \mu_2^2|H_2|^2 - [\mu_{12}^2 H_1^\dagger H_2 + \text{H.c.}] \\ & + \frac{\lambda_1}{2}|H_1|^4 + \frac{\lambda_2}{2}|H_2|^4 + \lambda_3|H_1|^2|H_2|^2 \\ & + \lambda_4|H_1^\dagger H_2|^2 + \frac{1}{2}[\lambda_5 (H_1^\dagger H_2)^2 + \text{H.c.}], \end{aligned} \tag{1}$$

and V_a the potential involving the pseudoscalar singlet field a,

$$\begin{aligned} V_a = {} & \frac{\mu_a^2}{2}a^2 + \frac{\lambda_a}{4}a^4 + (i\kappa a H_1^\dagger H_2 + \text{H.c.}) \\ & + \lambda_{aH_1} a^2|H_1|^2 + \lambda_{aH_2} a^2|H_2|^2. \end{aligned} \tag{2}$$

CP conservation in the scalar sector at zero temperature imposes that the field a have a vanishing vev $\langle a\rangle = 0$ in the EW vacuum, requiring

$$\mu_a^2 + (\lambda_{aH_1} v_1^2 + \lambda_{aH_2} v_2^2) = \mu_a^2 + \lambda_\beta v^2 \equiv m_a^2 > 0, \tag{3}$$

with $v_{1,2} = \sqrt{2}\langle H_{1,2}\rangle$ the vevs for the Higgs doublets after EW symmetry breaking (EWSB), $v = \sqrt{v_1^2 + v_2^2} = 246$ GeV the EW scale and $\lambda_\beta \equiv (\lambda_{aH_1} + \lambda_{aH_2} t_\beta^2)/(1 + t_\beta^2)$, with $t_\beta \equiv \tan\beta = v_2/v_1$.

In addition to the 125 GeV Higgs boson h, the physical scalar spectrum of the (CP-conserving) 2HDM contains a CP-even neutral state H_0, a CP-odd neutral state A_0 and a charged scalar $H^\pm$. Upon EWSB, the coupling κ in V_a induces a mixing between a and A_0, giving rise to two mass eigenstates, which we denote by $a_{1,2}$ (with $m_{a_2} > m_{a_1}$). The corresponding singlet-doublet mixing angle θ is given by (see, e.g., [29,31,32]) $t_{2\theta} = 2\kappa v/(m_{A_0}^2 - m_a^2)$, with m_{A_0} the 2HDM A_0 mass. In the rest of this work we consider the 2HDM alignment limit [36] (favored by current LHC Higgs signal strength measurements [37,38]), in which an angle β rotation of the CP-even neutral 2HDM field directions $h_{1,2}$ yields the CP-even Higgs mass eigenstates h and H_0. In addition we fix for simplicity a common mass scale M for the 2HDM states $H^\pm$, H_0 and A_0: $m_{H_0}^2 = m_{A_0}^2 = m_{H^\pm}^2 = M^2 \equiv \mu_{12}^2/(s_\beta c_\beta)$ (with $s_\beta \equiv \sin\beta$, $c_\beta \equiv \cos\beta$).

III. EARLY UNIVERSE THERMAL HISTORY

The spontaneous breaking of CP in the early Universe requires a negative mass-squared term for the singlet field a in (2),

$$\mu_a^2 = s_\theta^2 m_{a_2}^2 + c_\theta^2 m_{a_1}^2 - \lambda_\beta v^2 < 0. \tag{4}$$

Since $\mu_a^2 < 0$, the extrema along the $h_{1,2} = 0$, $a \neq 0$ field direction of the scalar potential at zero temperature lie away from the origin of field space, at $\langle a\rangle = \pm v_S \equiv \pm\sqrt{|\mu_a^2|/\lambda_a}$. For

$$(\lambda_{aH_1} v_S^2 + \mu_1^2)(\lambda_{aH_2} v_S^2 + \mu_2^2) > \mu_{12}^4 + \kappa^2 v_S^2, \tag{5}$$

these are minima of the tree-level scalar potential (otherwise they are saddle points). We also require that the EW vacuum be the absolute vacuum of the theory, which yields

$$-\mu_a^2 = \lambda_\beta v^2 - s_\theta^2 m_{a_2}^2 - c_\theta^2 m_{a_1}^2 < (m_h^2 v^2)/(2v_S^2). \tag{6}$$

This yields a lower bound on m_{a_1}, given by

$$m_{a_1,\rm min}^2 = ([\lambda_\beta - m_h^2/(2v_S^2)]c_\theta^2 v^2 - s_\theta^2 M^2)/(c_\theta^2 - s_\theta^2) \tag{7}$$

and is automatically satisfied when the $\langle a\rangle$ extrema are saddle points.

The combined dynamics of the two Higgs doublets $H_{1,2}$ and the singlet field a in the early Universe allows for a period of spontaneous CP breaking ending with the EW phase transition: First, the singlet develops a nonzero vev $v_S(T)$ at a temperature T_S, with the EW symmetry remaining unbroken. Then, EW symmetry breaking occurs at a lower temperature T_h, yielding a transition from the CPV minimum $(\langle h_1\rangle, \langle h_2\rangle, \langle a\rangle) = (0, 0, v_S(T))$ to the EW minimum $(v_1(T), v_2(T), 0)$, and restoring CP in the scalar sector. This two-step symmetry breaking process can be described to a good approximation by keeping only the tree-level potential V and the leading, $\mathcal{O}(T^2)$ thermal corrections in a high-temperature expansion of the 1-loop finite-temperature effective potential $V_{\rm eff}$ (see e.g. [39] for a review). The effective potential at $\mathcal{O}(T^2)$ has the advantage of manifestly avoiding issues related to the gauge-dependence of $V_{\rm eff}$, unlike the case with further contributions included [40]. In this paper, we keep our analysis at this order, leaving a study with the full 1-loop finite-temperature effective potential, including higher-order daisy contributions, for future work [35]. The $\mathcal{O}(T^2)$ thermal corrections are given by

$$V_T = \frac{T^2}{24}\sum_b n_b M_b^2 + \frac{T^2}{48}\sum_f n_f M_f^2 \tag{8}$$

with $M_b(h_1, h_2, a)$ and $M_f(h_1, h_2, a)$ respectively the field-dependent masses for bosons and fermions, and n_i the

number of degrees of freedom of each species. Summing up the dominant contributions of the top quark, the W and Z gauge bosons, the 2HDM scalars $H^{\pm}$, A_0, H_0 and h, the Goldstone bosons $G^{\pm}$ and G_0, and the singlet a, V_T reads (after dropping the field-independent contributions)

$$V_T = \frac{T^2}{24}\left[\left(2\lambda_3+\lambda_4+\frac{6m_W^2+3m_Z^2}{v^2}\right)(h_1^2+h_2^2) + (3\lambda_a+4\lambda_{aH_1}+4\lambda_{aH_2})a^2+(3\lambda_1+\lambda_{aH_1})h_1^2 + \left(3\lambda_2+\lambda_{aH_2}+\frac{6m_t^2(1+t_\beta^{-2})}{v^2}\right)h_2^2\right]. \quad (9)$$

Then, as the temperature of the early Universe decreases during radiation domination, the temperature T_S at which the singlet field direction gets destabilized (from the origin of field space) is given by $T_S^2 = 12|\mu_a^2|/(4\lambda_{aH_1}+4\lambda_{aH_2}+3\lambda_a)$. The Higgs field directions get instead destabilized at a temperature T_h given by $T_h^2 \simeq 6m_h^2v^2/(5m_h^2+\lambda_\beta v^2+6m_W^2+3m_Z^2+6m_t^2)$. Requiring $T_S > T_h$, for the spontaneous breaking of CP to occur prior to EW symmetry breaking, yields a lower bound on $|\mu_a^2|$ which by virtue of (4) can be cast as an upper bound on m_{a_1}:

$$m_{a_1,\max}^2 = \frac{1}{c_\theta^2-s_\theta^2}[c_\theta^2 v^2\lambda_\beta(1-F)-s_\theta^2M^2] \quad (10)$$

with

$$F = \frac{(4\lambda_{aH_1}+4\lambda_{aH_2}+3\lambda_a)m_h^2}{2(5m_h^2+\lambda_\beta v^2+6m_W^2+3m_Z^2+6m_t^2)}. \quad (11)$$

The combination of Eqs. (7) and (10) then defines a specific region of the 2HDM + a parameter space where a period of spontaneous CP violation would take place in the early Universe. This region is shown in Fig. 1 in the (λ_β, m_{a_1}) plane, for fixed M and s_θ, and two values of v_S (we take here the singlet self-coupling λ_a as a dependent parameter, subject to the perturbativity constraint $\lambda_a < 2\pi$).

Within the parameter space defined by Eqs. (7) and (10), there exists a *critical temperature* T_c at which the CPV $(0,0,v_S(T))$ and EW $(v_1(T),v_2(T),0)$ extrema become degenerate. The interplay between tree-level and $\mathcal{O}(T^2)$ terms in the 1-loop finite-temperature effective potential generally gives rise to a potential barrier between the two extrema [25] at T_c, which may result in a very strong first-order EW phase transition,[2] as needed for EW

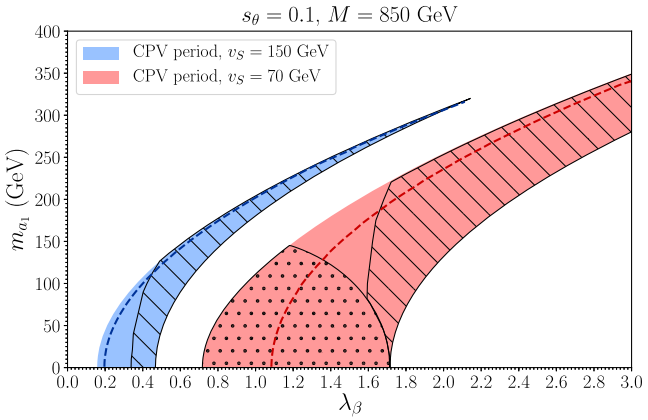

FIG. 1. m_{a_1} range leading to a spontaneous CP-breaking period prior to the EW phase transition, as a function of λ_β for $s_\theta = 0.1$, $M = 850$ GeV and $v_S = 150$ GeV (blue), $v_S = 70$ GeV (red), respectively. The regions to the right of the corresponding dashed lines feature $\xi_c \gtrsim 1$ as needed for EW baryogenesis (see text for details). In the bar-hatched regions, the Universe is trapped in the CPV minimum (no T_n exists). For the dot-hatched region, the CPV and EW extrema are saddle points at T_c at $\mathcal{O}(T^2)$ (see footnote 2).

baryogenesis. The tunneling from the CPV to the EW minimum takes place at the *nucleation temperature* $T_n < T_c$, and we must ensure that tunneling does occur (i.e., the Universe does not stay trapped in the singlet vacuum, see, e.g., [41,42] for recent discussions) for EW symmetry breaking to occur and our scenario to be physically viable. To verify this is the case, we implement the 2HDM + a in the numerical code CosmoTransitions [43]. The unphysical region for which the Universe becomes trapped in the CPV minimum (and no T_n exists) is shown as bar-hatched in Fig. 1.

The strength of the transition (which quantifies the departure from thermal equilibrium) can be characterized by the parameters $\xi_{c(n)} = v_{c(n)}/T_{c(n)}$, with $v_{c(n)}$ the value of the EW vev at $T_{c(n)}$. Successful baryogenesis requires $\xi_n \gtrsim 1$, to avoid baryon number washout. Except for the strongest transitions, ξ_c gives a good estimate of ξ_n, and we use the former in our discussion below (leaving a more detailed analysis for the future). Note that this approximation underestimates the relevant strength of the phase transition and the corresponding baryon asymmetry [see the discussion around Eq. (15)].

IV. *CP* VIOLATION

CP violation in the scalar sector is encoded in the phase of quantities that are rephasing invariant under $U(1)$ transformations of the Higgs doublets, e.g., $\lambda_5^*(\mu_{12}^2)^2$ in the 2HDM [44]. For $\lambda_5 = 0$ (following from our $m_{H_0}^2 \simeq m_{A_0}^2 \simeq m_{H^\pm}^2 = M^2$ simplifying assumption) there is thus no CP violation in the 2HDM scalar sector. In contrast, in the

[2]For the dot-hatched parameter regions of Fig. 1, at $\mathcal{O}(T^2)$ in the effective potential the CPV and EW extrema are actually saddle points at T_c. The inclusion of further 1-loop contributions (e.g., Coleman-Weinberg) does however lift both saddle points by creating a potential barrier between them, still resulting in a first-order EW phase transition [35]. We thus retain those shaded regions as potentially baryogenesis-viable in the present analysis.

2HDM + a, the presence of the $aH_1^\dagger H_2$ term in V yields the additional physical CP-violating phase $\delta_\kappa = \mathrm{Arg}[\kappa^* \mu_{12}^2]$. For $\mu_{12}^2, \kappa \in \mathbb{R}$ (so that $\delta_\kappa = 0$) the scalar sector of the 2HDM + a conserves CP in the EW minimum and there are no contributions to EDMs beyond the SM. Yet, even in this case a nonzero singlet vev $\langle a \rangle = v_S(T)$ generates transient CP violation via a complex squared-mass coefficient $\mu_{12}^2(T)$ for the $H_1^\dagger H_2$ term in (1),

$$\mu_{12}^2(T) = \mu_{12}^2 - i\kappa v_S(T). \tag{12}$$

The CP-violating phase $\delta_S = \mathrm{Arg}[\mu_{12}^2(T)^* \mu_{12}^2]$ is physical, signaling a nonremovable phase difference between vacua (here, the CPV minimum and the EW minimum) with different values of $v_S(T)$.

Expressing the neutral components of the Higgs doublets in radial form,

$$h_1 + i\zeta_1 = \eta_1 e^{i\theta_1}, \qquad h_2 + i\zeta_2 = \eta_2 e^{i\theta_2}, \tag{13}$$

only the combination $\theta = (\theta_1 - \theta_2)$ appears in the scalar potential V. The variation of θ during the EW phase transition due to the trajectory in field space between the CPV and EW minima[3] leads to the pseudoscalar component of the two Higgs doublets acquiring a transient nonzero value, before settling in the usual EW minimum at zero-temperature. The net change in θ across the EW phase transition precisely corresponds to δ_S. It is convenient to rotate the pair of Higgs doublets into the so-called "Higgs-basis" [36], where only one of the doublets acquires a vev at zero-temperature, in contrast to the "$\mathbb{Z}_2$-basis," where the softly-broken discrete symmetry is manifest but both doublets participate in EWSB. The rotation is achieved by the angle β and the analogous nonlinear representation defines (recall that we are working in the 2HDM alignment limit):

$$h + ig = \rho_1 e^{i\delta_1}, \qquad H_0 + iA_0 = \rho_2 e^{i\delta_2}, \tag{14}$$

where the imaginary components of the doublets now correspond to the would-be neutral Goldstone mode and the 2HDM pseudoscalar, respectively. The physical phase in this case is given by $\delta = (\delta_1 - \delta_2)$. The (4-dimensional) field trajectory between the CPV and EW minima is formally determined by finding the "bounce" solution that extremizes the Euclidean action, yet it is well approximated by the field trajectory which minimizes the effective potential. Here, we obtain that trajectory numerically by tracing along the straight line between the two minima in (ρ_1, a) space, and minimizing along the three remaining field directions. In Fig. 2 (top) we show isocontours of the effective potential at $T = T_c$ in the (ρ_1, a) plane for a chosen benchmark.

[3]Strictly speaking, θ is not defined at the CPV minimum, since both Higgs vevs are zero. However, it is well-defined by its limiting value, as the field trajectory tends to the CPV minimum.

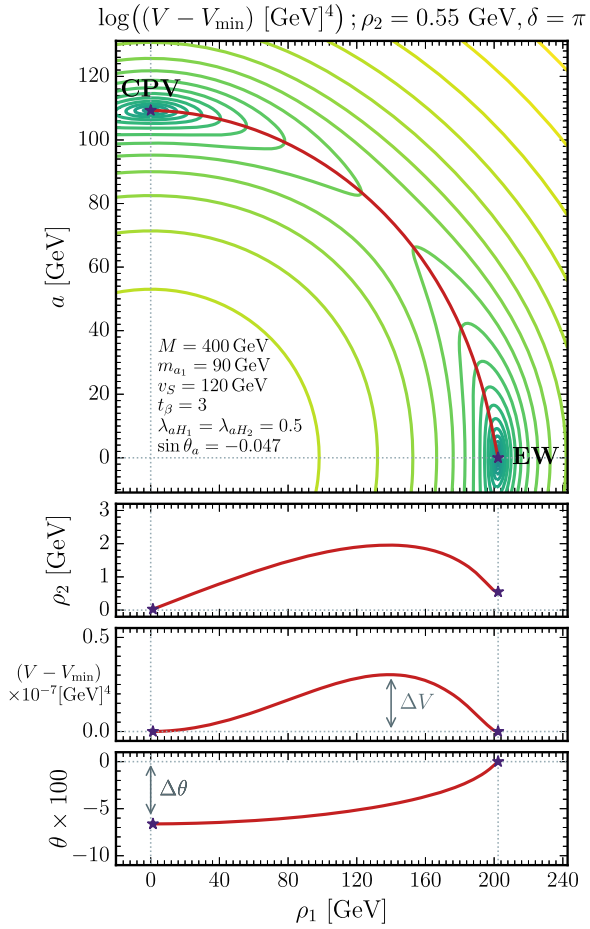

FIG. 2. Visualization of the potential in (ρ_1, a) space, for a benchmark point in our simplified scenario, with $M = 400$ GeV, $m_{a_1} = 90$ GeV, $v_S = 120$ GeV, $\lambda_{aH_1} = \lambda_{aH_2} = 0.5$, $t_\beta = 3$ and $\sin\theta = -0.047$. The potential is evaluated at $T = T_c$, fixing the values of ρ_2 and δ to their minima (0.55 GeV and π, respectively) in the EW phase. The path in field space that minimizes the effective potential is shown in red. The insets show the variation along this trajectory of the second Higgs field, ρ_2, the value of the potential and the relative phase between the two doublet fields in the $\mathbb{Z}_2$ basis, θ (See text for details).

The variation of several quantities along the field space trajectory as a function of ρ_1 are shown in the subfigures. The top subfigure shows the variation of the modulus of the second doublet, ρ_2. The middle subfigure shows the value of the potential, and hence the shape of the potential barrier between the two minima. The bottom subfigure shows the variation of θ and hence the amount of transient CP-violation generated during the phase transition. This is characterized by the change in θ, $\Delta\theta = \delta_S$, between the CPV and EW minima.

V. BARYOGENESIS

Electroweak baryogenesis is driven by CP-violating interactions of the SM fermions with the expanding

Higgs bubble walls (similarly to what occurs in baryogenesis within the 2HDM [45,46]). This generates chiral densities of quarks which diffuse into the symmetric phase in front of the bubbles. Electroweak sphalerons then produce a net baryon number. In the setup considered here, the top quark is the relevant fermion, and we use the formalism presented in [47]. It used to be commonly assumed that successful baryogenesis would require subsonic bubble expansion to allow for efficient diffusion of chiral densities into the symmetric phase (as, e.g., done in [47]), but recently it was shown that this assumption is too restrictive [48,49], and baryogenesis is also possible for larger values of the bubble wall velocity v_W. Rather than solving the transport equations of [47] explicitly, we use the analytic approximation

$$\frac{\eta}{10^{-11}} \sim 6 \times 10^2 \frac{\sin(\delta_t)\xi_c^2}{L_W T_c} \tag{15}$$

where η is the baryon-to-entropy ratio (our measure of the generated BAU), L_W is the thickness of the bubble wall and δ_t is the variation of the complex phase of the top-quark mass along the bubble wall, which drives the baryogenesis process and is related to δ_S by $\delta_t = \delta_S/(1+t_\beta^2)$. Comparing with [47], (15) reproduces the full results to about a factor of 2 for $v_W \lesssim 0.2$, which is sufficient accuracy for our application. In the following we thus allow $\eta \in [\eta_{\rm OBS}/2, 2\eta_{\rm OBS}]$, with $\eta_{\rm OBS}$ the observed BAU $\eta_{\rm OBS} = 8.7 \times 10^{-11}$ [50]. The results of [47] are based on a derivative expansion of the transport equations so require a sufficiently thick bubble wall, $L_W T_c \gtrsim 2$, which we find to be generically satisfied across the parameter space we study.

On general grounds, from the results of [48,49] one expects a mild suppression of the BAU (∼50%) compared to (15) for $0.2 \lesssim v_W \lesssim 0.5$, while for even larger wall velocities the suppression may become more severe. A detailed assessment of the impact of v_W on our BAU estimates is however beyond the scope of this work, and we use the approximation (15) in its present form.

In Fig. 4 we show in the (m_{a_1}, s_θ) plane two representative 2HDM + a baryogenesis benchmarks, given by $M =$ 400 GeV, $v_S = 130$ GeV, $t_\beta = 3$, $\lambda_{aH_2} = 5\lambda_{aH_1} = 0.5$ (in Type-I 2HDM, see [51]), and $M = 800$ GeV, $v_S =$ 130 GeV, $t_\beta = 2$, $\lambda_{aH_2} = \lambda_{aH_1} = 0.5$ (in Type-II 2HDM), depicted respectively in Fig. 4—top and Fig. 4—bottom. In each case, the region yielding $\eta \in [\eta_{\rm OBS}/2, 2\eta_{\rm OBS}]$ is shown as a red band. The benchmarks in Fig. 4—top never feature a potential barrier between the EW minimum and the CPV extrema at $T = 0$ (since Eq. (5) is never satisfied), and thus T_n is guaranteed to exist within our approximations. In contrast, for the benchmarks in Fig. 4—bottom, there is a set of m_{a_1} vs s_θ values that would yield $\eta = \eta_{\rm OBS}$ based on our analysis at T_c but for which no T_n exists (and is thus unphysical). These are depicted in Fig. 4 as a dotted-red line.

At this point, we reflect on the fact that the scalar potential V_a presents an unbroken $\mathbb{Z}_2$ symmetry under which $a \to -a$ (with either H_1 or H_2 being also odd under the $\mathbb{Z}_2$). When a develops a vev, there will not be a bias between transitions to $-v_S(T)$ and $+v_S(T)$, which would hinder viable baryogenesis: the volume of the regions with $+v_S(T)$ and $-v_S(T)$ would be essentially equal, and the baryon asymmetry generated in the regions with $+v_S(T)$ would be canceled out by that generated in the regions with $-v_S(T)$, since $\delta_S \propto \text{sign}[\pm v_S(T)]$. The result would be a vanishing net average baryon asymmetry over a Hubble volume, in spite of (15) locally yielding the observed baryon-to-entropy ratio.

This issue is solved by a small explicit $\mathbb{Z}_2$ breaking term in V_a, e.g. $(\mu_3/3)a^3$. Such a term would introduce a bias between the two singlet vacua, given by

$$\Delta V = \frac{\mu_3(\mu_3^2 + \lambda_a\mu_a^2)\sqrt{\mu_3^2 + 4\lambda_a\mu_a^2}}{6\lambda_a^3} \simeq \mu_3 v_S(T)^3 \tag{16}$$

where in the last step we have assumed $\mu_3^2 \ll \lambda_a\mu_a^2$ near the onset of the EW phase transition. In the presence of ΔV, the space-time regions with the deeper singlet minimum engulf those with the higher singlet minimum in a Hubble time, $t \sim H^{-1}$, provided that $\sigma/\Delta V \ll H^{-1}$ [15,52], with σ the surface tension of the domain-wall network. The time interval between the singlet and EW transitions in our model is in general much larger than H^{-1}. Then, then amount of bias ΔV needed for the (deeper) minimum to be the only vacuum remaining when the EW phase transition takes place is tiny (see also the discussion in [21])

$$\frac{\Delta V}{T^4} \simeq \frac{\mu_3 v_S(T)^3}{T^4} \gg 10^{-16}. \tag{17}$$

At the same time, from the properties of a, it is clear that *CP* breaking and $\mathbb{Z}_2$ breaking are connected: an a^3 term in V_a would lead to an explicit breaking of *CP* in the scalar potential, and so the radiative generation of a nonzero μ_3 is (only) possible via an explicit breaking of *CP* in $V_{\rm 2HDM} + V_a$, e.g. through a complex μ_{12}^2 term (when κ is real). This term would generate μ_3 at 1-loop (see Figure 3), of order

$$\begin{aligned}\mu_3 &\sim \int \frac{d^4p}{(4\pi)^2} \frac{\max(\lambda_{aH_1}, \lambda_{aH_2})\kappa|\mu_{12}^2|\sin\delta_{12}}{(p^2 - M^2)^3} \\ &\sim \frac{\max(\lambda_{aH_1}, \lambda_{aH_2})\kappa|\mu_{12}^2|\sin\delta_{12}}{16\pi^2 M^2},\end{aligned} \tag{18}$$

with δ_{12} the phase of the μ_{12}^2 term for real κ. For $\max(\lambda_{aH_1}, \lambda_{aH_2}) \sim \mathcal{O}(1)$, $\sin\theta \ll 1$ (such that $\kappa \sim \sin\theta \times M^2/v$), $|\mu_{12}^2| \sim M^2$ and $v_S(T) \sim T$, the condition (17) for viable baryogenesis translates into

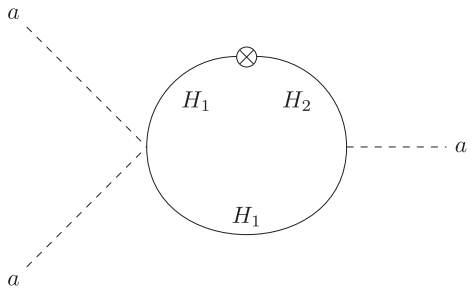

FIG. 3. 1-loop contribution to the CP-breaking term a^3, proportional to λ_{aH_1}. The $\otimes$ symbol represents an insertion of the μ_{12}^2 mass term from V_{2HDM}.

$$\sin\delta_{12} \gg 10^{-16} \times \frac{(16\pi^2)vT}{M^2} \sim 10^{-15} \tag{19}$$

where a mild hierarchy between M and both v and T_n has been assumed in the last step of (19). The required amount of explicit CP-violation is therefore unobservably small. It will have no impact on the *local* baryon asymmetry generated in the vicinity of the bubble walls [Eq. (15)], serving only to ensure that this asymmetry is translated into a *global* one (over a Hubble volume) by preferring a particular sign for the singlet vacuum in the early universe.

In this respect, it has been recently pointed out [53] that, given that CP is violated in the SM by the fermion sector, this will inevitably leak to the scalar sector, and renormalizability of the 2HDM at the 3-loop level does seem to require a complex μ_{12}^2, i.e. a nonzero value of δ_{12}. Assuming a 3-loop suppression combined with the SM Jarlskog invariant suppression for the generated δ_{12} yields $\sin\delta_{12} \sim 10^{-12}$, very far below current and foreseen EDM experimental sensitivity (see, e.g., [44,46]) but still above what is needed to satisfy (19). Thus, it is plausible that CP violation in the SM quark sector, leaking to the 2HDM scalar sector (as recently discussed in [53]) can actually generate the required bias in V_a for successful baryogenesis. In any case, a very small amount of explicit CP breaking in the 2HDM scalar sector, far below foreseen EDM experimental sensitivity (see, e.g.. [44,46]) is enough to provide the required bias for successful baryogenesis, and CP is approximately conserved at present in the scalar sector.

VI. PHENOMENOLOGICAL IMPLICATIONS

The landmark phenomenological signatures of the scenario investigated in this work are the existence of a light pseudoscalar a_1 (with $m_{a_1} < v$) accompanied by a (2HDM-like) set of spin-0 states around/below the TeV scale (recall that $m_{H_0} \simeq M$, and Eq. (10) imposes $M < v\sqrt{\lambda_\beta}/t_\theta$ to obtain $m_{a_1,\max} > 0$), with cascade decays into a_1, e.g., $H_0 \to Za_1$, $H_0 \to a_1a_1$, $a_2 \to ha_1$ and $H^\pm \to W^\pm a_1$. In Fig. 4 we show the current experimental limits and future

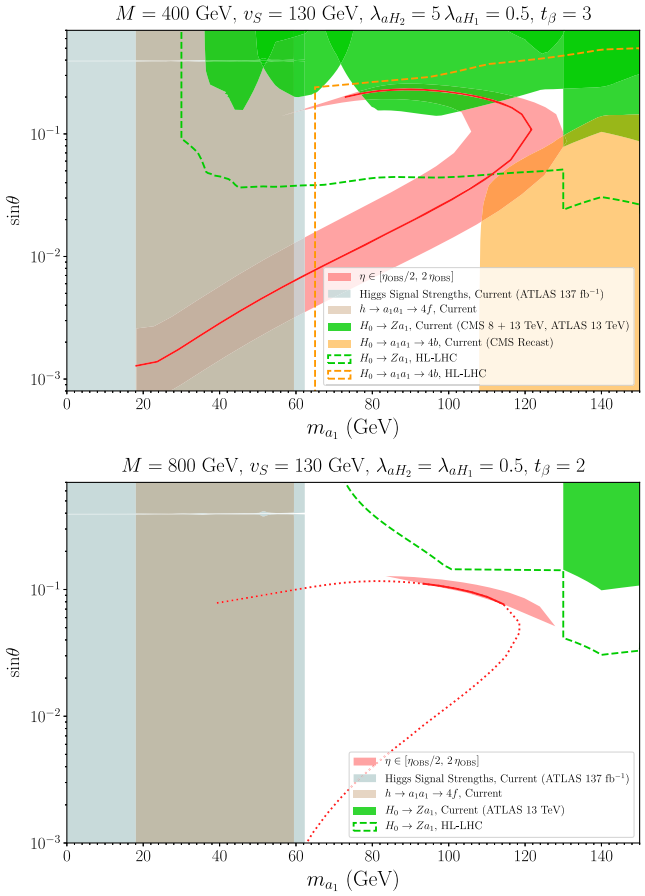

FIG. 4. (m_{a_1}, s_θ) plane for the benchmarks $M = 400$ GeV, $v_S = 130$ GeV, $t_\beta = 3$, $\lambda_{aH_2} = 5\lambda_{aH_1} = 0.5$ in Type-I 2HDM (top panel) and $M = 800$ GeV, $v_S = 130$ GeV, $t_\beta = 2$, $\lambda_{aH_2} = \lambda_{aH_1} = 0.5$ in Type-II 2HDM (bottom panel). The red band corresponds to $\eta \in [\eta_{\text{OBS}}/2, 2\eta_{\text{OBS}}]$, with $\eta = \eta_{\text{OBS}}$ shown as a solid red line. Parameter values that would yield $\eta = \eta_{\text{OBS}}$ (based on an analysis at T_c) but for which no T_n exists (thus being unphysical) are shown as a dotted red line. Solid colored regions (green, gray, brown, yellow) correspond to present experimentally excluded regions by LHC searches, while the dashed-colored lines show the future HL-LHC 95% C.L. exclusion sensitivity in each case.

sensitivity to the two representative 2HDM + a baryogenesis benchmarks discussed above, in the m_{a_1} vs s_θ plane. The mass region $m_{a_1} < m_h/2$ is very strongly constrained by both LHC measurements of the 125 GeV Higgs signal strengths [54] and direct searches for exotic Higgs boson decays $h \to a_1a_1 \to 4f$ (f being SM fermions), e.g., in the $b\bar{b}\tau\tau$ and $b\bar{b}\mu\mu$ final states (see [55] for an up-to-date review of these searches). These probe the branching fraction $\text{BR}(h \to a_1a_1)$ (proportional to $\lambda_\beta^2 c_\theta^4$ and whose explicit expression in terms of the 2HDM + a parameters can be found in [32]), and Fig. 4 shows the corresponding present 95% C.L. limits.

The specific interplay among different experimental probes of the light pseudoscalar a_1 in LHC cascade decays (when available by phase-space) heavily depends on the value of s_θ. The decay widths for $H_0 \to Za_1$, $a_2 \to ha_1$ and $H^\pm \to W^\pm a_1$ are proportional to s_θ^2, and thus such channels may become suppressed for $s_\theta \ll 1$. Yet, in this limit the decay width for $H_0 \to a_1 a_1$ scales as $(\lambda_{aH_1} - \lambda_{aH_2})^2 c_\theta^4$ [32] and could thus lead to a large BR for $\lambda_{aH_1} \neq \lambda_{aH_2}$. In particular, for $|\lambda_{aH_1} - \lambda_{aH_2}| \gtrsim 0.1$, $H_0 \to a_1 a_1$ can be the dominant decay channel of H_0, and would constitute an important probe of the $s_\theta \ll 1$ baryogenesis regime. Ref [56] has recently performed an LHC sensitivity study of the channel $pp \to H_0 \to a_1 a_1 \to b\bar{b}b\bar{b}$ by recasting the latest di-Higgs CMS search in the $4b$ final state [57]. We here use `SusHi` [58] to obtain the NNLO production cross section for H_0 and show in Fig. 4 the present 95% C.L. limit from searches for the $pp \to H_0 \to Za_1 \to \ell\ell\bar{b}b$ channel by CMS [59,60] and ATLAS [61], and searches for $pp \to H_0 \to a_1 a_1 \to b\bar{b}b\bar{b}$ (from the recast performed in [56]). We also show the expected 95% C.L. sensitivity of all these searches at the HL-LHC as dashed lines. For the benchmark in Fig. 4—top, the combination of these searches with Higgs signal strength measurements will be able to probe the whole region of viable baryogenesis. This is however not entirely so for the benchmark in Fig. 4—bottom, for which $\lambda_{aH_1} = \lambda_{aH_2}$ and thus $H_0 \to a_1 a_1$ searches do not provide sensitivity. We also find that other LHC searches for a_1 (e.g., direct production in gluon-fusion followed by the a_1 decay into diphoton or ditau final states) and for H_0 (e.g. via $H_0 \to \tau\tau$ decays) do not provide meaningful constraints to the benchmarks considered in Fig. 4.

Finally, the viable baryogenesis parameter space is also constrained by flavor observables, particularly from rare B-meson decays: Existing constraints from $b \to s\gamma$ decays set a 95% C.L. limit $m_{H^\pm} > 790$ GeV for Type-II 2HDM [62] (the specific value of this limit being currently under debate [63,64]), taken into account in our analysis. The existence of a light pseudoscalar state a_1 coupling to SM fermions could also be probed by its contributions to the decay $B_s \to \mu^+\mu^-$ [65,66], but only for Type-II 2HDM and $t_\beta \gg 1$, which would however suppress the generated BAU.

VII. COMMENT ON THE DM CONNECTION

The 2HDM + a model is a well-motivated DM portal, with the simple addition of a singlet Dirac fermion χ (the DM candidate) coupled to a through a Yukawa term $y_\chi a\bar{\chi}\gamma_5\chi$. Among its virtues, it naturally avoids spin-independent DM direct detection experimental limits (since a is a pseudoscalar mediator, see, e.g., [67]), and could explain the possible galactic center γ-ray excess [29,68,69]. Remarkably, there exists an interplay between baryogenesis and DM in this scenario: The coupling y_χ contributes to the effective potential, and its effect is included via $4\lambda_{aH_1} + 4\lambda_{aH_2} + 3\lambda_a \to 4\lambda_{aH_1} + 4\lambda_{aH_2} + 3\lambda_a + 2y_\chi^2$ in (11). Thus, it leads to a decrease in T_S and the corresponding shrinking of the parameter space region where spontaneous *CP* violation prior to the EW phase transition occurs. At the same time, the early Universe DM annihilation cross section for $\chi\bar{\chi} \to p_{\rm SM} p_{\rm SM}$ (with $p_{\rm SM}$ generic SM particles) processes leading to the observed DM relic density via thermal freeze-out scales as $\langle\sigma v\rangle \propto y_\chi^2 s_\theta^2 m_\chi^2/m_{a_1}^4$ (for $m_{a_1} \ll m_{a_2}$). With the rest of model parameters fixed, the value of y_χ yielding the observed DM relic density scales as s_θ^{-2}, leading to a minimum value of s_θ compatible with the DM relic density and yielding spontaneous *CP* violation prior to the EW phase transition (i.e., with $T_S > T_h$). We will explore this interplay in detail and the possibility of achieving baryogenesis and the correct relic DM abundance in this scenario in an upcoming work [35].

VIII. CONCLUSIONS

We have proposed a variant of electroweak baryogenesis characterized by the spontaneous breaking of *CP* in the early Universe, driven by the vev of a *CP*-odd scalar a. Working in a specific realization of such a setup, given by a 2HDM + a extended Higgs sector, we have shown that this *CP*-breaking period, followed by a strongly first-order electroweak phase transition, is able to generate the observed baryon asymmetry of the Universe in sizable regions of the parameter space of the model, while naturally avoiding the stringent EDM experimental constraints on BSM *CP*-violating sources. The existence of such a *CP*-breaking period in the early Universe generally demands the existence of a singlet-like light *CP*-odd scalar (necessarily coupled to the SM fermions (via its mixing with the Higgs doublets) to ensure viable baryogenesis. This light pseudo-scalar can be searched for at the LHC, dominantly in cascade decays of the heavier 2HDM scalars (and also possibly via low-energy flavor measurements), yielding a powerful probe of our proposed scenario. Finally, we stress that the electroweak phase transition in this setup is rather strong in general, and would possibly lead to a stochastic gravitational wave signal in the observable range of the future LISA observatory [70], a study we intend to carry out in the future.

ACKNOWLEDGMENTS

Feynman diagrams were drawn using TikZ-Feynman [71]. S. J. H. is supported by the Science Technology and Facilities Council (STFC) under Consolidated Grant No. ST/T00102X/1. K. M. is supported by the UK STFC via Grant No. ST/T000759/1. The work of J. M. N. is supported by the Ramón y Cajal Fellowship contract No. RYC-2017-22986, and by Grant No. PGC2018-096646-A-I00 from the

Spanish Proyectos de I + D de Generación de Conocimiento. J. M. N. also acknowledges support from the European Union's Horizon 2020 research and innovation programme under the Marie Sklodowska-Curie Grant agreement No. 860881 (ITN HIDDeN), as well as from the grant IFT Centro de Excelencia Severo Ochoa No. CEX2020-001007-S funded by No. MCIN/AEI/10.13039/501100011033.

[1] N. Cabibbo, Phys. Rev. Lett. **10**, 531 (1963).
[2] M. Kobayashi and T. Maskawa, Prog. Theor. Phys. **49**, 652 (1973).
[3] V. A. Kuzmin, V. A. Rubakov, and M. E. Shaposhnikov, Phys. Lett. **155B**, 36 (1985).
[4] A. D. Sakharov, Pis'ma Zh. Eksp. Teor. Fiz. **5**, 32 (1967).
[5] A. G. Cohen, D. B. Kaplan, and A. E. Nelson, Annu. Rev. Nucl. Part. Sci. **43**, 27 (1993).
[6] M. Trodden, Rev. Mod. Phys. **71**, 1463 (1999).
[7] D. E. Morrissey and M. J. Ramsey-Musolf, New J. Phys. **14**, 125003 (2012).
[8] T. Konstandin, Phys. Usp. **56**, 747 (2013).
[9] M. B. Gavela, P. Hernandez, J. Orloff, and O. Pene, Mod. Phys. Lett. A **9**, 795 (1994).
[10] M. B. Gavela, M. Lozano, J. Orloff, and O. Pene, Nucl. Phys. **B430**, 345 (1994).
[11] M. B. Gavela, P. Hernandez, J. Orloff, O. Pene, and C. Quimbay, Nucl. Phys. **B430**, 382 (1994).
[12] V. Andreev *et al.* (ACME Collaboration), Nature (London) **562**, 355 (2018).
[13] C. Abel *et al.* (nEDM Collaboration), Phys. Rev. Lett. **124**, 081803 (2020).
[14] W. C. Griffith, M. D. Swallows, T. H. Loftus, M. V. Romalis, B. R. Heckel, and E. N. Fortson, Phys. Rev. Lett. **102**, 101601 (2009).
[15] J. R. Espinosa, B. Gripaios, T. Konstandin, and F. Riva, J. Cosmol. Astropart. Phys. 01 (2012) 012.
[16] J. M. Cline and K. Kainulainen, J. Cosmol. Astropart. Phys. 01 (2013) 012.
[17] I. Baldes, T. Konstandin, and G. Servant, Phys. Lett. B **786**, 373 (2018).
[18] J. M. Cline, K. Kainulainen, and D. Tucker-Smith, Phys. Rev. D **95**, 115006 (2017).
[19] M. Carena, M. Quirós, and Y. Zhang, Phys. Rev. Lett. **122**, 201802 (2019).
[20] E. Hall, T. Konstandin, R. McGehee, H. Murayama, and G. Servant, J. High Energy Phys. 04 (2020) 042.
[21] W. Chao, Phys. Lett. B **796**, 102 (2019).
[22] L. Biermann, M. Mühlleitner, and J. Müller, arXiv: 2204.13425.
[23] J. M. Cline and P.-A. Lemieux, Phys. Rev. D **55**, 3873 (1997).
[24] S. Profumo, M. J. Ramsey-Musolf, and G. Shaughnessy, J. High Energy Phys. 08 (**2007**) 010.
[25] J. R. Espinosa, T. Konstandin, and F. Riva, Nucl. Phys. **B854**, 592 (2012).
[26] G. C. Dorsch, S. J. Huber, and J. M. No, J. High Energy Phys. 10 (2013) 029.
[27] P. Basler, M. Krause, M. Muhlleitner, J. Wittbrodt, and A. Wlotzka, J. High Energy Phys. 02 (2017) 121.
[28] G. Dorsch, S. Huber, K. Mimasu, and J. No, J. High Energy Phys. 12 (2017) 086.
[29] S. Ipek, D. McKeen, and A. E. Nelson, Phys. Rev. D **90**, 055021 (2014).
[30] J. M. No, Phys. Rev. D **93**, 031701 (2016).
[31] D. Goncalves, P. A. N. Machado, and J. M. No, Phys. Rev. D **95**, 055027 (2017).
[32] M. Bauer, U. Haisch, and F. Kahlhoefer, J. High Energy Phys. 05 (2017) 138.
[33] T. Abe *et al.* (LHC Dark Matter Working Group), Phys. Dark Universe **27**, 100351 (2020).
[34] T. Robens, Symmetry **13**, 2341 (2021).
[35] S. J. Huber, K. Mimasu, and J. M. No (to be published).
[36] J. F. Gunion and H. E. Haber, Phys. Rev. D **67**, 075019 (2003).
[37] CMS Collaboration, Report No. CMS-PAS-HIG-19-005, 2020.
[38] ATLAS Collaboration, Report No. ATLAS-CONF-2020-027, 2020.
[39] M. Quiros, arXiv:hep-ph/9901312.
[40] H. H. Patel and M. J. Ramsey-Musolf, J. High Energy Phys. 07 (2011) 029.
[41] S. Baum, M. Carena, N. R. Shah, C. E. M. Wagner, and Y. Wang, J. High Energy Phys. 03 (2021) 055.
[42] T. Biekötter, S. Heinemeyer, J. M. No, M. O. Olea, and G. Weiglein, J. Cosmol. Astropart. Phys. 06 (2021) 018.
[43] C. L. Wainwright, Comput. Phys. Commun. **183**, 2006 (2012).
[44] S. Inoue, M. J. Ramsey-Musolf, and Y. Zhang, Phys. Rev. D **89**, 115023 (2014).
[45] L. Fromme, S. J. Huber, and M. Seniuch, J. High Energy Phys. 11 (2006) 038.
[46] G. Dorsch, S. Huber, T. Konstandin, and J. No, J. Cosmol. Astropart. Phys. 05 (2017) 052.
[47] L. Fromme and S. J. Huber, J. High Energy Phys. 03 (2007) 049.
[48] J. M. Cline and K. Kainulainen, Phys. Rev. D **101**, 063525 (2020).
[49] G. C. Dorsch, S. J. Huber, and T. Konstandin, J. Cosmol. Astropart. Phys. 08 (2021) 020.
[50] P. A. R. Ade *et al.* (Planck Collaboration), Astron. Astrophys. **594**, A13 (2016).
[51] G. C. Branco, P. M. Ferreira, L. Lavoura, M. N. Rebelo, M. Sher, and J. P. Silva, Phys. Rep. **516**, 1 (2012).
[52] J. McDonald, Phys. Lett. B **357**, 19 (1995).
[53] D. Fontes, M. Löschner, J. C. Romão, and J. a. P. Silva, Eur. Phys. J. C **81**, 541 (2021).

[54] ATLAS Collaboration, Report No. ATLAS-CONF-2021-053, 2021.
[55] M. Cepeda, S. Gori, V. M. Outschoorn, and J. Shelton, arXiv:2111.12751.
[56] D. Barducci, K. Mimasu, J. M. No, C. Vernieri, and J. Zurita, J. High Energy Phys. 02 (2020) 002.
[57] A. M. Sirunyan *et al.* (CMS Collaboration), J. High Energy Phys. 08 (2018) 152.
[58] R. V. Harlander, S. Liebler, and H. Mantler, Comput. Phys. Commun. **184**, 1605 (2013).
[59] V. Khachatryan *et al.* (CMS Collaboration), Phys. Lett. B **759**, 369 (2016).
[60] CMS Collaboration, Report No. CMS-PAS-HIG-18-012, 2019.
[61] M. Aaboud *et al.* (ATLAS Collaboration), Phys. Lett. B **783**, 392 (2018).
[62] O. Atkinson, M. Black, A. Lenz, A. Rusov, and J. Wynne, J. High Energy Phys. 04 (**2022**) 172.
[63] T. Hermann, M. Misiak, and M. Steinhauser, J. High Energy Phys. 11 (2012) 036.
[64] M. Misiak, A. Rehman, and M. Steinhauser, J. High Energy Phys. 06 (2020) 175.
[65] W. Skiba and J. Kalinowski, Nucl. Phys. **B404**, 3 (1993).
[66] H. E. Logan and U. Nierste, Nucl. Phys. **B586**, 39 (2000).
[67] A. De Simone and T. Jacques, Eur. Phys. J. C **76**, 367 (2016).
[68] D. Hooper and L. Goodenough, Phys. Lett. B **697**, 412 (2011).
[69] D. Hooper and T. Linden, Phys. Rev. D **84**, 123005 (2011).
[70] C. Caprini *et al.*, J. Cosmol. Astropart. Phys. 03 (2020) 024.
[71] J. Ellis, Comput. Phys. Commun. **210**, 103 (2017).